 CMC, vol.1, no.3, pp.245-258, 2004

A Matrix Decomposition MFS Algorithm for Biharmonic Problems in Annular Domains

T. Tsangaris[1], Y.–S. Smyrlis[1,2] and A. Karageorghis[1,2]

Abstract: The Method of Fundamental Solutions (MFS) is a boundary-type method for the solution of certain elliptic boundary value problems. In this work, we develop an efficient matrix decomposition MFS algorithm for the solution of biharmonic problems in annular domains. The circulant structure of the matrices involved in the MFS discretization is exploited by using Fast Fourier Transforms. The algorithm is tested numerically on several examples.

keyword: Method of fundamental solutions, biharmonic equation, circulant matrices, annular domains, fast Fourier transform.

1 Introduction

The Method of Fundamental Solutions (MFS) is a meshless technique for the numerical solution of certain elliptic and parabolic differential equations (Fairweather and Karageorghis (1998); Golberg and Chen (2001); Cho, Golberg, Muleshkov, and Li (2004)). It is applicable when the fundamental solution of the elliptic operator in question is known. In the MFS, singularities of the fundamental solution, are avoided by the introduction of a fictitious boundary exterior to the problem geometry (the *pseudo–boundary*). Thus the approximate solution satisfies the underlying partial differential equation. Since the method was first introduced by Kupradze and Aleksidze (1963, 1964), and was first proposed as a numerical technique by Mathon and Johnston (1977), it has been applied to a wide variety of physical problems.

In recent years, this boundary–type technique has become very popular because of its simplicity and ease of numerical implementation. Details concerning the various aspects and applications of the MFS can be found in the recent survey papers by Cho, Golberg, Muleshkov, and Li (2004); Fairweather and Karageorghis (1998); Fairweather, Karageorghis, and Martin (2003); Golberg and Chen (1997, 1999); Kołodziej (2001).

There are various formulations of the MFS. The two most popular ones are the following: In the first one, the singularities are fixed, whereas in the second one they are determined as part of the solution of the discrete problem. The latter, which results in a nonlinear least–squares problem, was used for the solution of biharmonic problems in Karageorghis and Fairweather (1987, 1988, 1989). In particular, in Karageorghis and Fairweather (1987), the authors used the integral representation of Maiti and Chakrabarty (1974), while in Karageorghis and Fairweather (1989) the authors used the simple layer potential representation of Fichera (1961) and in Karageorghis and Fairweather (1988) the authors used the Almansi representation of biharmonic functions, introduced by Almansi (1897). The above studies reveal that these three formulations can be implemented equally easily and that there is little to choose between them with respect to accuracy.

The MFS with fixed singularities, which results in a linear system, was used for the solution of biharmonic problems in circular domains in Smyrlis and Karageorghis (2003). This version of the MFS was also used for the solution of three–dimensional biharmonic problems in axisymmetric domains in Fairweather, Karageorghis, and Smyrlis (2004). In this study, we shall be using the MFS with fixed singularities for the solution of biharmonic problems in annular domains. We shall be extending the ideas used in Smyrlis and Karageorghis (2003) as well as in Tsangaris, Smyrlis, and Karageorghis (2004), where the MFS was used for the solution of harmonic problems in annular domains. A variant of the MFS involving Green's functions was applied to the solution of harmonic problems in annular domains in Katsurada (1989).

In this work we shall be using the properties of circu-

[1] Department of Mathematics & Statistics, University of Cyprus, Nicosia, Cyprus. (Τμήμα Μαθηματικών & Στατιστικής, Πανεπιστήμιο Κύπρου, Λευκωσία, Κύπρος)

[2] Supported by a University of Cyprus grant.

lant matrices. The occurrence of such matrices when the MFS is applied to circular domains was first observed by Katsurada and Okamoto (1988). The properties of the circulant matrices resulting from the MFS discretization, in conjunction with the use of the Fast Fourier Transform (FFT), were fully exploited in Smyrlis and Karageorghis (2001, 2004b) for harmonic problems and in Smyrlis and Karageorghis (2003) for biharmonic problems. It is noteworthy that with the use of FFTs the computational effort is reduced from $O(N^3)$ operations to $O(N\log N)$ operations. The properties of circulant matrices in conjunction with the Boundary Element Method (BEM) were also studied by Jeng–Tzong Chen and his co–workers in Chen, Lin, Kuo, and Chyuan (2001); Kuo, Chen, and Huang (2000).

2 MFS formulation

We consider the boundary value problem

$$\begin{cases} \Delta^2 u = 0 & \text{in} \quad \Omega, \\ u = f_1 \quad \text{and} \quad \dfrac{\partial u}{\partial n} = g_1 & \text{on} \quad \partial\Omega_1, \\ u = f_2 \quad \text{and} \quad \dfrac{\partial u}{\partial n} = g_2 & \text{on} \quad \partial\Omega_2, \end{cases} \tag{2.1}$$

where the domain Ω is the annulus

$$\Omega = \{\boldsymbol{x} \in \mathbb{R}^2 : \rho_1 < |\boldsymbol{x}| < \rho_2\}, \tag{2.2}$$

Δ denotes the Laplace operator and f_1, f_2, g_1 and g_2 are given functions. The boundary of Ω is $\partial\Omega = \partial\Omega_1 \cup \partial\Omega_2$ where $\partial\Omega_1$ and $\partial\Omega_2$ are the circles with radii ρ_1 and ρ_2, respectively.

The MFS biharmonic formulation we shall be using is based on the single layer potential representation of Maiti and Chakrabarty (1974) according to which, a biharmonic function in a sufficiently smooth bounded domain $\Omega \subset \mathbb{R}^2$, can be expressed as

$$\begin{aligned} u(P) = &\int_{\partial\Omega} \mu(Q)\log|P-Q|\, d\sigma(Q) \\ &+ \int_{\partial\Omega} \nu(Q)\,|P-Q|^2\big(\log|P-Q|-1\big)\, d\sigma(Q), \end{aligned} \tag{2.3}$$

where the functions μ and ν are *source densities* at the boundary.

In the MFS, we attempt to approximate the integral representation (2.3) by a quadrature rule. Thus the solution u is approximated by (see Bogomolny (1985); Fairweather and Karageorghis (1998); Murashima, Nonaka, and Nieda (1983); Smyrlis and Karageorghis (2003))

$$u_N(\boldsymbol{\mu},\boldsymbol{\nu},\boldsymbol{Q};P) = \sum_{j=1}^{2N} \big\{\mu_j k_1(P,Q_j) + \nu_j k_2(P,Q_j)\big\}, \tag{2.4}$$

where $\boldsymbol{\mu} = (\mu_1,\ldots,\mu_{2N})^T$, $\boldsymbol{\nu} = (\nu_1,\nu_2,\ldots,\nu_{2N})^T$ and $\mathbf{Q}$ is a $4N-$vector containing the coordinates of the singularities Q_j, $j = 1,\ldots,2N$, which lie outside $\overline{\Omega}$. The function $k_1(P,Q)$ is a fundamental solution of Laplace's equation given by

$$k_1(P,Q) = -\frac{1}{2\pi}\log|P-Q|, \tag{2.5}$$

and the function $k_2(P,Q)$ is a fundamental solution of the biharmonic equation given by

$$k_2(P,Q) = -\frac{1}{8\pi}|P-Q|^2\log|P-Q|. \tag{2.6}$$

It should be noted that the completeness of these bases is discussed in Bogomolny (1985).

The singularities Q_j are fixed on the pseudo–boundary $\partial\tilde{\Omega} = \partial\tilde{\Omega}_1 \cup \partial\tilde{\Omega}_2$ of an annulus $\tilde{\Omega}$ concentric to Ω and defined by

$$\tilde{\Omega} = \{\boldsymbol{x} \in \mathbb{R}^2 : R_1 < |\boldsymbol{x}| < R_2\},$$

where $R_2 > \rho_2 > \rho_1 > R_1$. The boundary of $\tilde{\Omega}$ comprises $\partial\tilde{\Omega}_1$ and $\partial\tilde{\Omega}_2$, the circles with radii R_1 and R_2, respectively.

A set of collocation points $\{P_i\}_{i=1}^{2N}$ is placed on $\partial\Omega$. If $P_i = (x_{P_i}, y_{P_i})$, then we take

$$\begin{aligned} x_{P_i} &= \rho_1 \cos\frac{2(i-1)\pi}{N}, \\ y_{P_i} &= \rho_1 \sin\frac{2(i-1)\pi}{N}, \end{aligned} \tag{2.7}$$

and

$$\begin{aligned} x_{P_{N+i}} &= \rho_2 \cos\frac{2(i-1)\pi}{N}, \\ y_{P_{N+i}} &= \rho_2 \sin\frac{2(i-1)\pi}{N}, \end{aligned} \tag{2.8}$$

where $i = 1,\ldots,N$. If $Q_j = (x_{Q_j}, y_{Q_j})$, then

$$\begin{aligned} x_{Q_j} &= R_1 \cos\frac{2(j-1+\alpha)\pi}{N}, \\ y_{Q_j} &= R_1 \sin\frac{2(j-1+\alpha)\pi}{N}, \end{aligned} \tag{2.9}$$

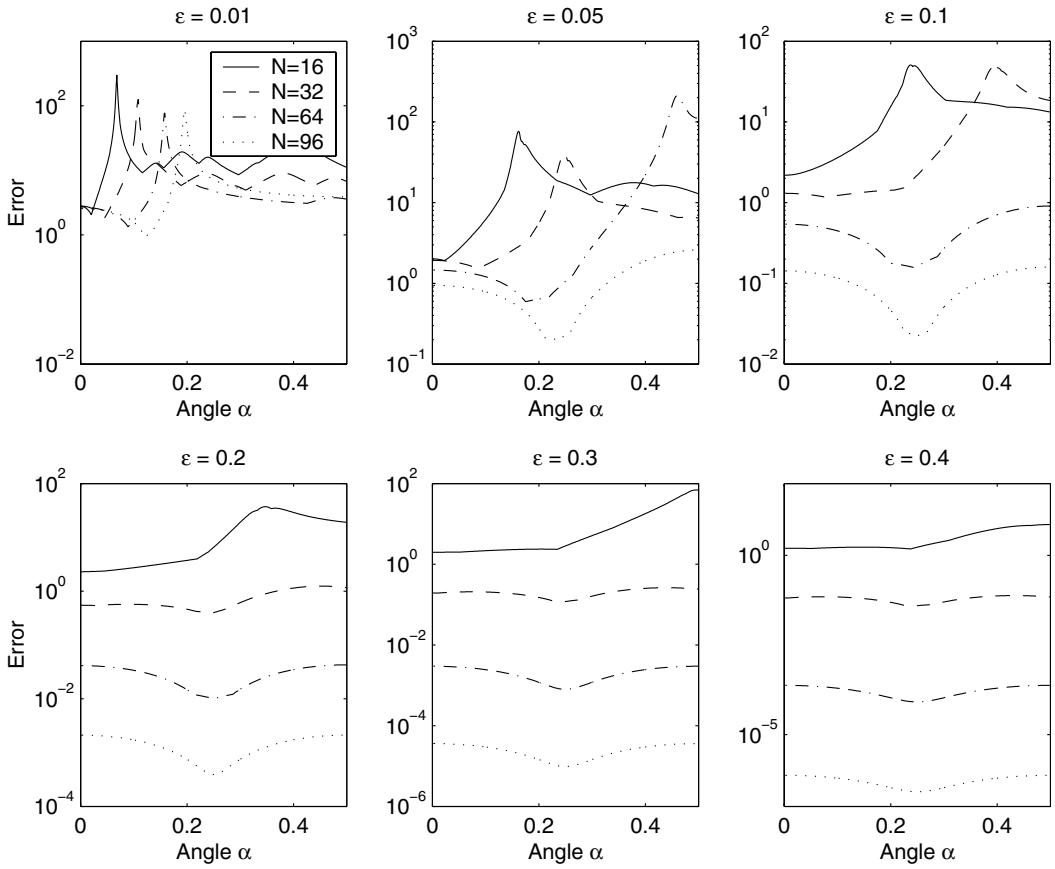

Figure 1 : Log–plot of error versus angular parameter α for ε in Example 1 for different values of N.

and

$$x_{Q_{N+j}} = R_2 \cos \frac{2(j-1+\alpha)\pi}{N},$$
$$y_{Q_{N+j}} = R_2 \sin \frac{2(j-1+\alpha)\pi}{N}, \tag{2.10}$$

where $j = 1,\ldots,N$.

The presence of the angular parameter $\alpha \in [-\frac{1}{2}, \frac{1}{2}]$ indicates that the sources are rotated by an angle $2\pi\alpha/N$ with respect to the boundary points. This rotation is known to improve the accuracy of the approximation significantly when the pseudo–boundary is very close to the boundary. (See Smyrlis and Karageorghis (2001, 2004b)).

The vectors of coefficients $\boldsymbol{\mu}$ and $\boldsymbol{\nu}$ are determined so that the boundary conditions are satisfied at the collocation points $\{P_i\}_{i=1}^{2N}$:

$$u_N(\boldsymbol{\mu},\boldsymbol{\nu},\boldsymbol{Q};P_i) = f_1(P_i),$$
$$\frac{\partial}{\partial n} u_N(\boldsymbol{\mu},\boldsymbol{\nu},\boldsymbol{Q};P_i) = g_1(P_i), \tag{2.11}$$

and

$$u_N(\boldsymbol{\mu},\boldsymbol{\nu},\boldsymbol{Q};P_{N+i}) = f_2(P_{N+i}),$$
$$\frac{\partial}{\partial n} u_N(\boldsymbol{\mu},\boldsymbol{\nu},\boldsymbol{Q};P_{N+i}) = g_2(P_{N+i}), \tag{2.12}$$

for $i = 1,\ldots,N$, where $\partial/\partial n$ is exterior normal derivative on the boundary $\partial\Omega$. This yields a linear system of the form

$$\left(\begin{array}{c|c|c|c} A_{11} & A_{12} & A_{13} & A_{14} \\ \hline A_{21} & A_{22} & A_{23} & A_{24} \\ \hline A_{31} & A_{32} & A_{33} & A_{34} \\ \hline A_{41} & A_{42} & A_{43} & A_{44} \end{array}\right) \left(\begin{array}{c} \boldsymbol{s}_1 \\ \hline \boldsymbol{s}_2 \\ \hline \boldsymbol{t}_1 \\ \hline \boldsymbol{t}_2 \end{array}\right) = \left(\begin{array}{c} \boldsymbol{f}_1 \\ \hline \boldsymbol{f}_2 \\ \hline \boldsymbol{g}_1 \\ \hline \boldsymbol{g}_2 \end{array}\right), \tag{2.13}$$

where

$$\boldsymbol{s}_1 = (\mu_1,\mu_2,\ldots,\mu_N)^T,\ \boldsymbol{s}_2 = (\mu_{N+1},\mu_{N+2},\ldots,\mu_{2N})^T,$$
$$\boldsymbol{t}_1 = (\nu_1,\nu_2,\ldots,\nu_N)^T,\ \boldsymbol{t}_2 = (\nu_{N+1},\nu_{N+2},\ldots,\nu_{2N})^T.$$

The elements of the matrices A_{mn}, $m,n = 1,\cdots,4$ are

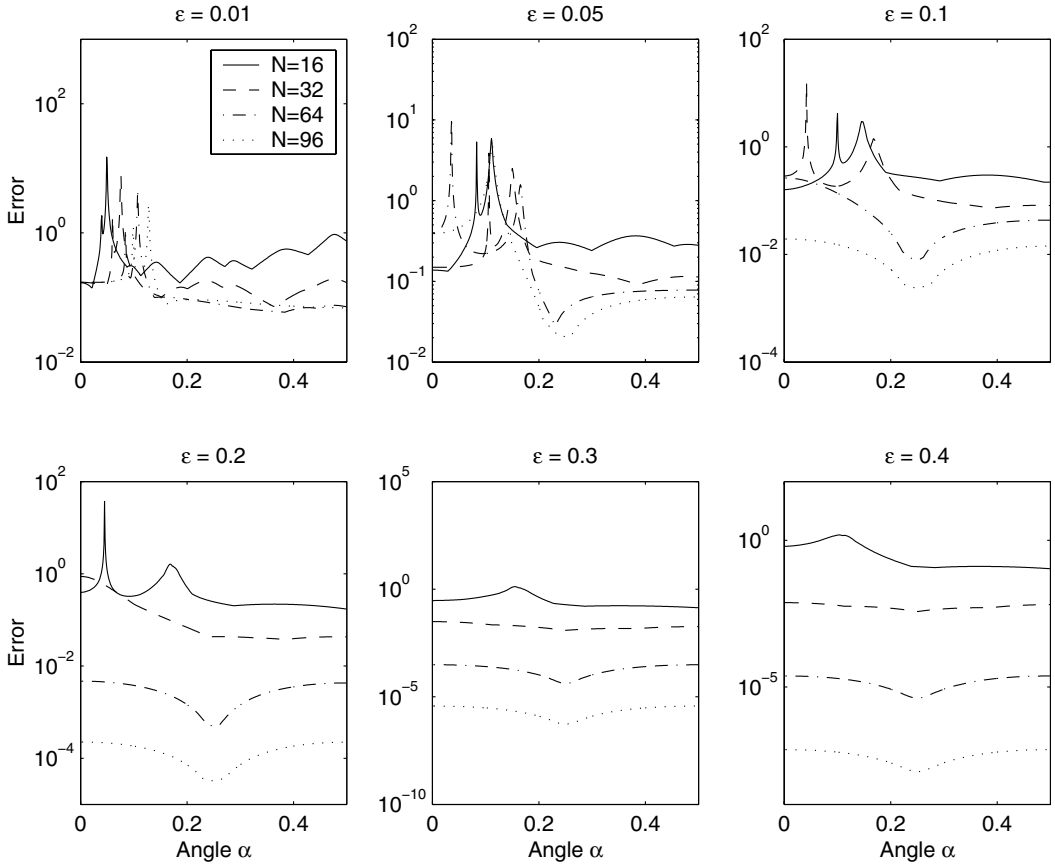

Figure 2 : Log–plot of error versus angular parameter α for ε in Example 2 for different values of N.

given by

$$
\begin{aligned}
&(A_{11})_{i,j} = k_1(P_i,Q_j), \qquad (A_{12})_{i,j} = k_1(P_i,Q_{N+j}),\\
&(A_{13})_{i,j} = k_2(P_i,Q_j), \qquad (A_{14})_{i,j} = k_2(P_i,Q_{N+j}),\\
&(A_{21})_{i,j} = k_1(P_{N+i},Q_j), \qquad (A_{22})_{i,j} = k_1(P_{N+i},Q_{N+j}),\\
&(A_{23})_{i,j} = k_2(P_{N+i},Q_j), \qquad (A_{24})_{i,j} = k_2(P_{N+i},Q_{N+j}),\\
&(A_{31})_{i,j} = h_1(P_i,Q_j), \qquad (A_{32})_{i,j} = h_1(P_i,Q_{N+j}),\\
&(A_{33})_{i,j} = h_2(P_i,Q_j), \qquad (A_{34})_{i,j} = h_2(P_i,Q_{N+j}),\\
&(A_{41})_{i,j} = h_1(P_{N+i},Q_j), \qquad (A_{42})_{i,j} = h_1(P_{N+i},Q_{N+j}),\\
&(A_{43})_{i,j} = h_2(P_{N+i},Q_j), \qquad (A_{44})_{i,j} = h_2(P_{N+i},Q_{N+j}),
\end{aligned}
$$

for $i,j = 1,\ldots,N$, with

$$
\begin{aligned}
k_1(\boldsymbol{x},\boldsymbol{y}) &= -\frac{1}{2\pi}\log|\boldsymbol{x}-\boldsymbol{y}|,\\
k_2(\boldsymbol{x},\boldsymbol{y}) &= -\frac{1}{8\pi}|\boldsymbol{x}-\boldsymbol{y}|^2\log|\boldsymbol{x}-\boldsymbol{y}|,
\end{aligned}
$$

and

$$
\begin{aligned}
h_1(\boldsymbol{x},\boldsymbol{y}) &= -\frac{1}{2\pi}\frac{(\boldsymbol{x}-\boldsymbol{y})\cdot\boldsymbol{x}}{|\boldsymbol{x}||\boldsymbol{x}-\boldsymbol{y}|^2},\\
h_2(\boldsymbol{x},\boldsymbol{y}) &= -\frac{1}{8\pi}\big(1+2\log|\boldsymbol{x}-\boldsymbol{y}|\big)\frac{(\boldsymbol{x}-\boldsymbol{y})\cdot\boldsymbol{x}}{|\boldsymbol{x}|},
\end{aligned}
$$

where $\boldsymbol{x}$ and $\boldsymbol{y}$ are the vectors describing the points P and Q, respectively. The functions h_1 and h_2 are the normal derivatives of k_1 and k_2, respectively, with direction extrerior to the boundary, i.e.,

$$
h_j(\boldsymbol{x},\boldsymbol{y}) = \nabla_{\boldsymbol{x}} k_j(\boldsymbol{x},\boldsymbol{y})\cdot\boldsymbol{n} = \frac{\partial}{\partial n(\boldsymbol{x})}k_j(\boldsymbol{x},\boldsymbol{y}), \quad j=1,2,
$$

where $\boldsymbol{n}$ is the unit normal exterior to the boundary of Ω. The matrices $A_{mn}, m,n = 1,\cdots,4$ are *circulant*[3] and thus

[3] A square matrix A is circulant (see Davis (1979)) if it has the form

$$
A = \begin{pmatrix} a_1 & a_2 & \cdots & a_N \\ a_N & a_1 & \cdots & a_{N-1} \\ \cdots & \cdots & \cdots & \cdots \\ a_2 & a_3 & \cdots & a_1 \end{pmatrix}. \tag{2.14}
$$

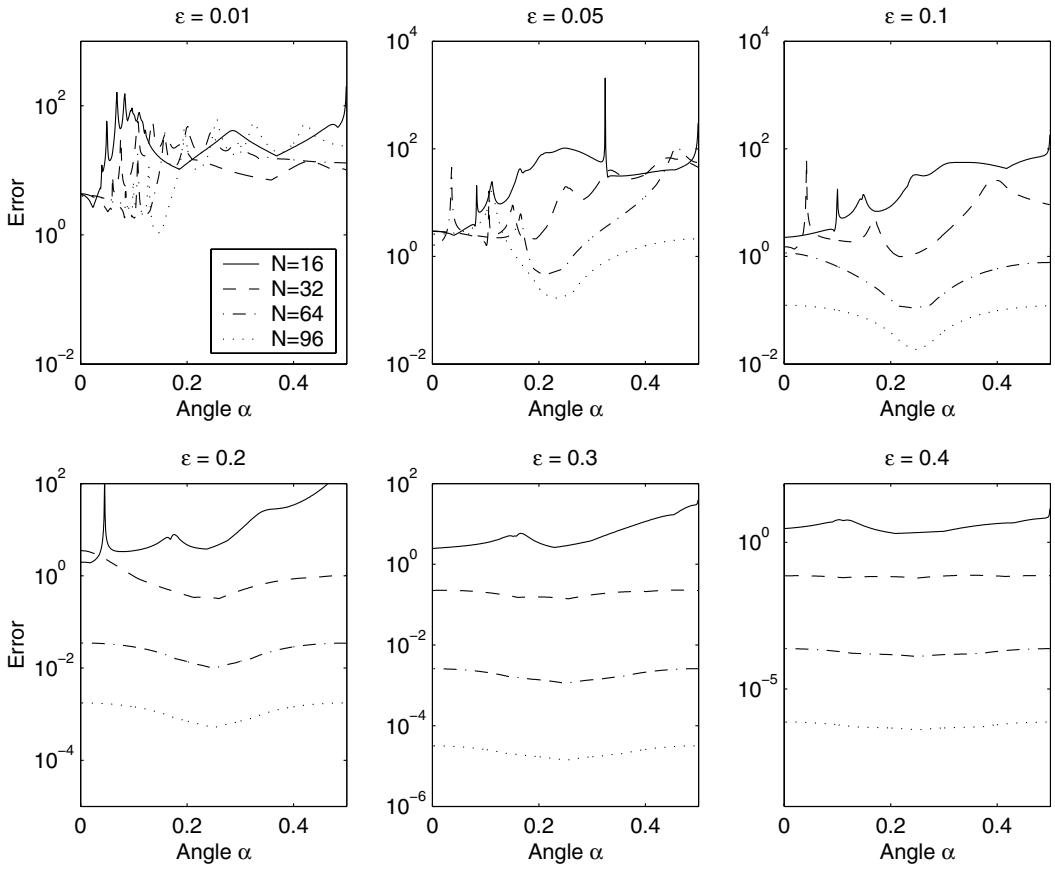

Figure 3 : Log–plot of error versus angular parameter α for ε in Example 3 for different values of N.

diagonalizable. In particular,

$$A_{mn} = U^* D_{mn} U, \quad m,n = 1,\ldots,4, \tag{2.15}$$

where

$$D_{mn} = \operatorname{diag}\left(\lambda_1^{mn},\ldots,\lambda_N^{mn}\right), \quad m,n = 1,\cdots,4,$$

are diagonal matrices whose diagonal elements are the eigenvalues of the matrices A_{mn}, $m,n = 1,\cdots,4$, respectively, and

$$U^* = \frac{1}{\sqrt{N}} \begin{pmatrix} 1 & 1 & 1 & \cdots & 1 \\ 1 & \omega & \omega^2 & \cdots & \omega^{N-1} \\ 1 & \omega^2 & \omega^4 & \cdots & \omega^{2N-2} \\ \cdots & \cdots & \cdots & \cdots & \cdots \\ 1 & \omega^{N-1} & \omega^{2(N-1)} & \cdots & \omega^{(N-1)(N-1)} \end{pmatrix},$$

with $\omega = e^{\frac{2\pi i}{N}}$. The matrix U^* is known as the Fourier matrix and it can be readily verified that it is unitary. If $A_{mn} = \operatorname{circ}\left(a_1^{mn},\ldots,a_N^{mn}\right)$, then the elements of the diagonal matrices D_{mn} are given by (see Davis (1979))

$$\lambda_j^{mn} = \sum_{\ell=1}^{N} \omega^{(j-1)(\ell-1)} a_\ell^{mn}.$$

Note that from the above expression it is obvious that the λ_j^{mn} can be obtained from the a_ℓ^{mn} via discrete Fourier transforms.

3 Matrix decomposition algorithm

Let

$$\hat{A} = (I_4 \otimes U) \left(\begin{array}{c|c|c|c} A_{11} & A_{12} & A_{13} & A_{14} \\ \hline A_{21} & A_{22} & A_{23} & A_{24} \\ \hline A_{31} & A_{32} & A_{33} & A_{34} \\ \hline A_{41} & A_{42} & A_{43} & A_{44} \end{array}\right) (I_4 \otimes U^*),$$

where I_4 is the identity matrix in $\mathbb{R}^{4\times 4}$ and $\otimes$ denotes the matrix tensor product. The system (2.13) can be written

This means that the elements of each row are same as the elements of the previous row but moved one position to the right. The first element of each row is the same as the the last element of the previous row. The circulant matrix A in (2.14) is usually denoted by $A = \operatorname{circ}(a_1, a_2, \ldots, a_N)$.

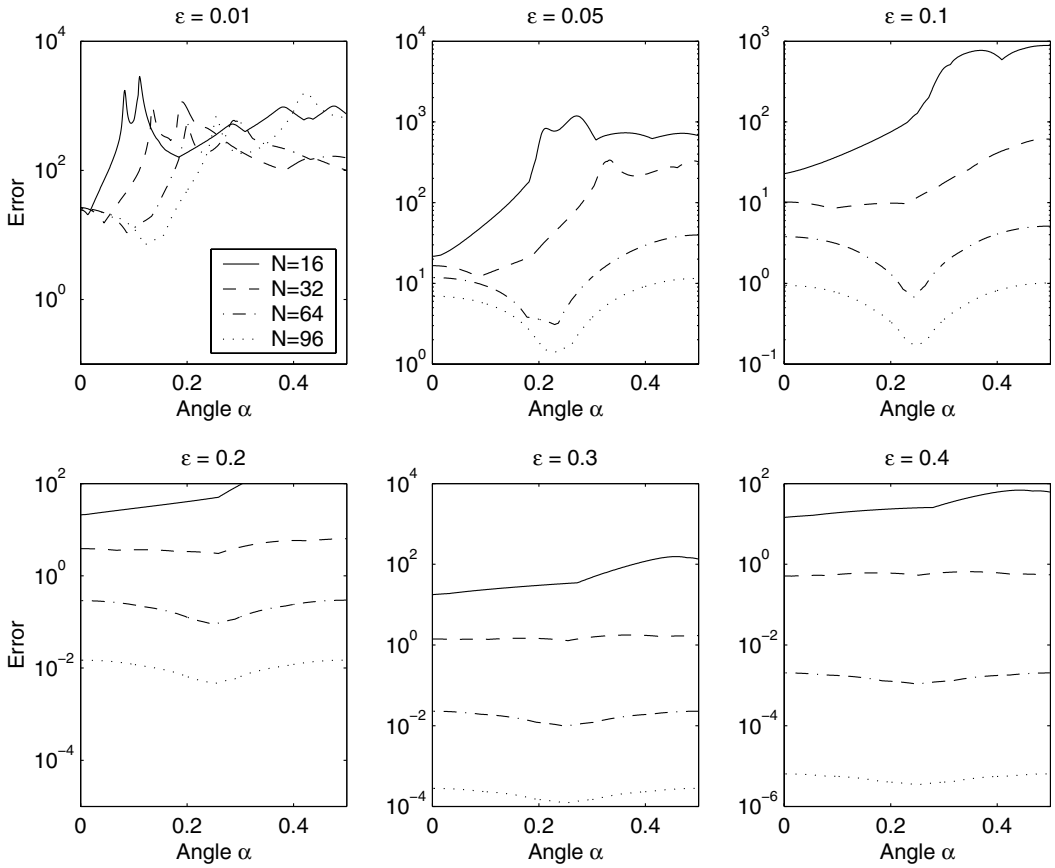

Figure 4 : Log–plot of error versus angular parameter α for ε in Example 4 for different values of N.

as

$$\hat{A}\,(I_4\otimes U)\begin{pmatrix}\boldsymbol{s}_1\\ \boldsymbol{s}_2\\ \boldsymbol{t}_1\\ \boldsymbol{t}_2\end{pmatrix}=(I_4\otimes U)\begin{pmatrix}\boldsymbol{f}_1\\ \boldsymbol{f}_2\\ \boldsymbol{g}_1\\ \boldsymbol{g}_2\end{pmatrix}, \tag{3.1}$$

where the matrix $\hat{A}$ can be written as

$$\hat{A} = \left(\begin{array}{c|c|c|c} UA_{11}U^* & UA_{12}U^* & UA_{13}U^* & UA_{14}U^* \\ \hline UA_{21}U^* & UA_{22}U^* & UA_{23}U^* & UA_{24}U^* \\ \hline UA_{31}U^* & UA_{32}U^* & UA_{33}U^* & UA_{34}U^* \\ \hline UA_{41}U^* & UA_{42}U^* & UA_{43}U^* & UA_{44}U^* \end{array}\right)$$

$$= \left(\begin{array}{c|c|c|c} D_{11} & D_{12} & D_{13} & D_{14} \\ \hline D_{21} & D_{22} & D_{23} & D_{24} \\ \hline D_{31} & D_{32} & D_{33} & D_{34} \\ \hline D_{41} & D_{42} & D_{43} & D_{44} \end{array}\right).$$

Also,

$$(I_4\otimes U)\begin{pmatrix}\boldsymbol{s}_1\\ \boldsymbol{s}_2\\ \boldsymbol{t}_1\\ \boldsymbol{t}_2\end{pmatrix}=\begin{pmatrix}U\boldsymbol{s}_1\\ U\boldsymbol{s}_2\\ U\boldsymbol{t}_1\\ U\boldsymbol{t}_2\end{pmatrix}=\begin{pmatrix}\hat{\boldsymbol{s}}_1\\ \hat{\boldsymbol{s}}_2\\ \hat{\boldsymbol{t}}_1\\ \hat{\boldsymbol{t}}_2\end{pmatrix}$$

and

$$(I_4\otimes U)\begin{pmatrix}\boldsymbol{f}_1\\ \boldsymbol{f}_2\\ \boldsymbol{g}_1\\ \boldsymbol{g}_2\end{pmatrix}=\begin{pmatrix}U\boldsymbol{f}_1\\ U\boldsymbol{f}_2\\ U\boldsymbol{g}_1\\ U\boldsymbol{g}_2\end{pmatrix}=\begin{pmatrix}\hat{\boldsymbol{f}}_1\\ \hat{\boldsymbol{f}}_2\\ \hat{\boldsymbol{g}}_1\\ \hat{\boldsymbol{g}}_2\end{pmatrix},$$

where

$$\hat{\boldsymbol{s}}_1=U\boldsymbol{s}_1,\ \hat{\boldsymbol{s}}_2=U\boldsymbol{s}_2,\ \hat{\boldsymbol{t}}_1=U\boldsymbol{t}_1,\ \hat{\boldsymbol{t}}_2=U\boldsymbol{t}_2,$$

$$\hat{\boldsymbol{f}}_1=U\boldsymbol{f}_1,\ \hat{\boldsymbol{f}}_2=U\boldsymbol{f}_2,\ \hat{\boldsymbol{g}}_1=U\boldsymbol{g}_1,\ \hat{\boldsymbol{g}}_2=U\boldsymbol{g}_2,$$

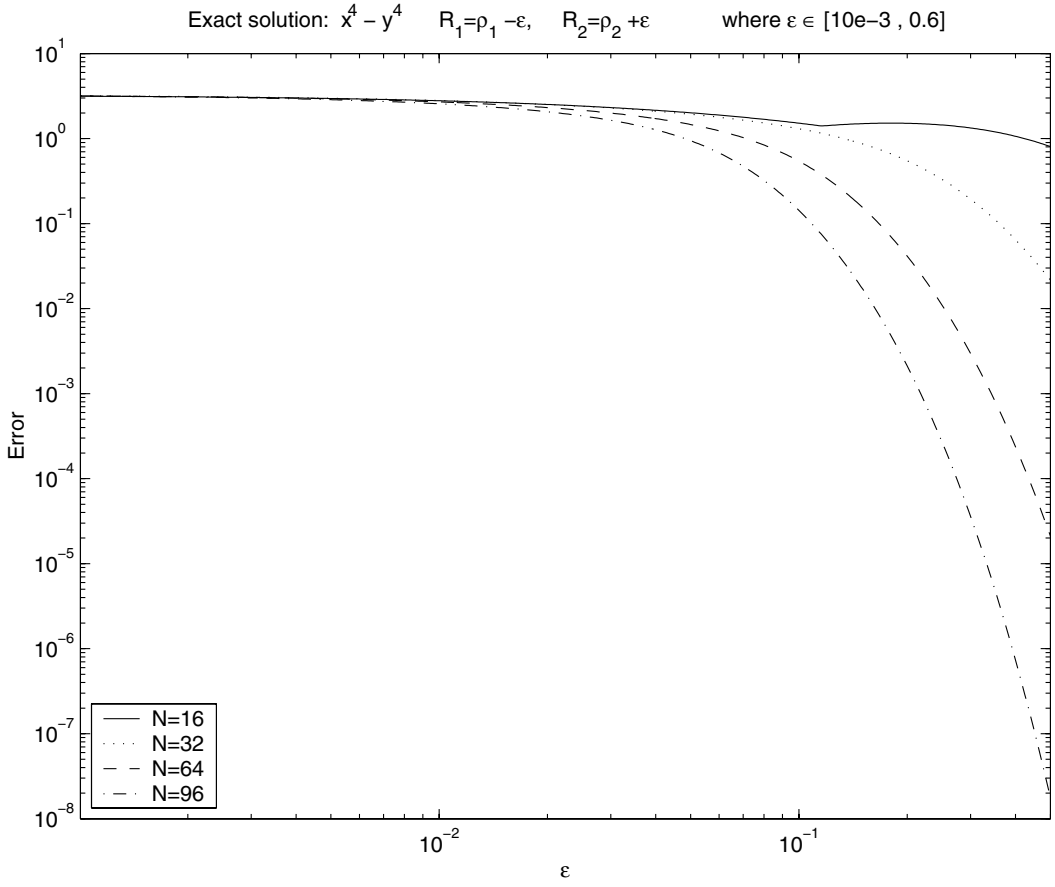

Figure 5 : Log–plot of maximum relative error versus ε in Example 1 for different values of N.

where $i = 1,2,\ldots,N$. Finally, system (3.1) is reduced to

$$\left(\begin{array}{c|c|c|c} D_{11} & D_{12} & D_{13} & D_{14} \\ \hline D_{21} & D_{22} & D_{23} & D_{24} \\ \hline D_{31} & D_{32} & D_{33} & D_{34} \\ \hline D_{41} & D_{42} & D_{43} & D_{44} \end{array}\right) \left(\begin{array}{c} \hat{\boldsymbol{s}}_1 \\ \hline \hat{\boldsymbol{s}}_2 \\ \hline \hat{\boldsymbol{t}}_1 \\ \hline \hat{\boldsymbol{t}}_2 \end{array}\right) = \left(\begin{array}{c} \hat{\boldsymbol{f}}_1 \\ \hline \hat{\boldsymbol{f}}_2 \\ \hline \hat{\boldsymbol{g}}_1 \\ \hline \hat{\boldsymbol{g}}_2 \end{array}\right), \quad (3.2)$$

The solution of system (3.2) can be decomposed into the solution of the N independent 4×4 systems

$$\begin{pmatrix} \lambda_i^{11} & \lambda_i^{12} & \lambda_i^{13} & \lambda_i^{14} \\ \lambda_i^{21} & \lambda_i^{22} & \lambda_i^{23} & \lambda_i^{24} \\ \lambda_i^{31} & \lambda_i^{32} & \lambda_i^{33} & \lambda_i^{34} \\ \lambda_i^{41} & \lambda_i^{42} & \lambda_i^{43} & \lambda_i^{44} \end{pmatrix} \begin{pmatrix} \hat{s}_i^1 \\ \hat{s}_i^2 \\ \hat{t}_i^1 \\ \hat{t}_i^2 \end{pmatrix} = \begin{pmatrix} \hat{f}_i^1 \\ \hat{f}_i^2 \\ \hat{g}_i^1 \\ \hat{g}_i^2 \end{pmatrix}, \quad (3.3)$$

where $i = 1,2,\ldots,N$. Having obtained $\hat{\boldsymbol{s}}_1,\hat{\boldsymbol{s}}_2$ and $\hat{\boldsymbol{t}}_1,\hat{\boldsymbol{t}}_2$, we can find $\boldsymbol{s}_1,\boldsymbol{s}_2$ and $\boldsymbol{t}_1,\boldsymbol{t}_2$, (and hence $\boldsymbol{\mu},\boldsymbol{\nu}$) from

$$\boldsymbol{s}_1 = U^*\hat{\boldsymbol{s}}_1, \quad \boldsymbol{s}_2 = U^*\hat{\boldsymbol{s}}_2, \quad \boldsymbol{t}_1 = U^*\hat{\boldsymbol{t}}_1, \quad \boldsymbol{t}_2 = U^*\hat{\boldsymbol{t}}_2.$$

We thus have the following matrix decomposition algorithm for solving (2.13):

Description of the algorithm

Step 1: Compute $\hat{\boldsymbol{f}}_1 = U\boldsymbol{f}_1$, $\hat{\boldsymbol{f}}_2 = U\boldsymbol{f}_2$ and $\hat{\boldsymbol{g}}_1 = U\boldsymbol{g}_1$, $\hat{\boldsymbol{g}}_2 = U\boldsymbol{g}_2$.

Step 2: Construct the diagonal matrices D_{mn}, $m,n = 1,\ldots,4$.

Step 3: Evaluate $\hat{\boldsymbol{s}}_1,\hat{\boldsymbol{s}}_2$ and $\hat{\boldsymbol{t}}_1,\hat{\boldsymbol{t}}_2$ by solving N 4×4 complex systems.

Step 4: Compute $\boldsymbol{s}_1 = U^*\hat{\boldsymbol{s}}_1$, $\boldsymbol{s}_2 = U^*\hat{\boldsymbol{s}}_2$ and $\boldsymbol{t}_1 = U^*\hat{\boldsymbol{t}}_1$, $\boldsymbol{t}_2 = U^*\hat{\boldsymbol{t}}_2$.

Analysis of the cost

(i) In ***Step* 1** and ***Step* 4**, because of the form of the matrices U and U^*, the operations can be carried out via FFTs at a cost of $O(N\log N)$ operations.

(ii) FFTs can also be used for the evaluation of the diagonal matrices in ***Step* 2**.

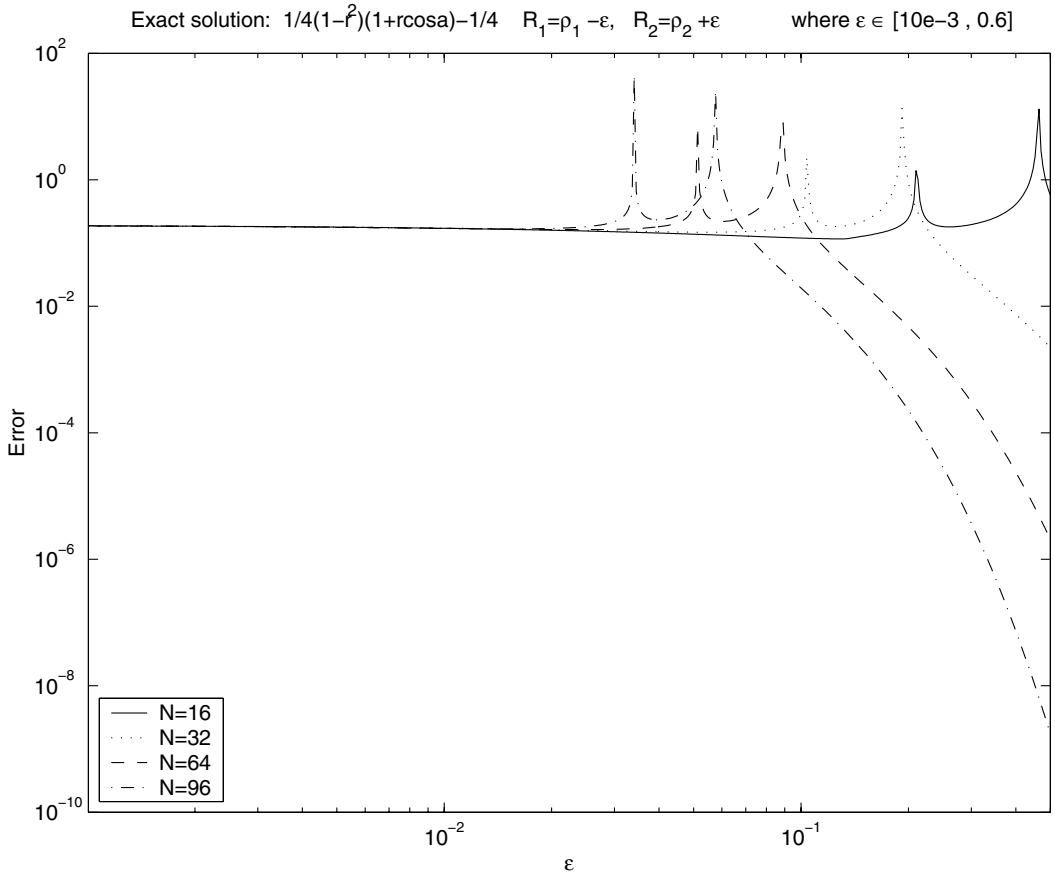

Figure 6 : Log–plot of maximum relative error versus ε in Example 2 for different values of N.

(iii) The FFT operations are performed using the NAG[4] routines `C06FPF`, `C06FQF` and `C06FRF`.

(iv) In ***Step*** **3**, we need to solve N complex linear systems of order 4. This is done at a cost of $O(N)$ operations using the NAG routine `F04ADF`.

Note. A similar algorithm can also be applied in the case of different combinations of boundary conditions associated with the biharmonic equation.

4 Numerical results

We considered the following numerical examples corresponding to the Dirichlet problem (2.1) in the annulus defined by $\rho_1 = 1$ and $\rho_2 = 2$:

Example 1. Problem corresponding to the exact solution $u(x,y) = x^4 - y^4$.

[4] Numerical Analysis Group (NAG) Library Mark 20, NAG Ltd, Wilkinson House, Jordan Hill Road, Oxford, UK, 2001.

Example 2. In this case we consider a test example from Kuwahara and Imai (1969), where in polar coordinates $f(\theta) = -\frac{1}{4}$ and $g(\theta) = -\frac{1}{2}(1+\cos\theta)$, which corresponds to the exact solution

$$u(r,\theta) = \frac{1}{4}(1-r^2)(1+r\cos\theta) - \frac{1}{4}.$$

Example 3. Problem corresponding to the exact solution

$$u(x,y) = (x^2+y^2)\,e^x \cos y + \frac{x}{x^2+y^2}.$$

Example 4. Problem corresponding to the exact solution

$$\begin{aligned} u(x,y) &= (x^2+y^2)\{(x+iy)^3 + (x-iy)^3\} \\ &\quad + \{(x+iy)^5 + (x-iy)^5\}. \end{aligned}$$

The maximum relative error in these examples was calculated on a grid of m^2 points on the annulus defined by $(r_i\cos\vartheta_j, r_i\sin\vartheta_j)$, with

$$r_i = \rho_1 + \frac{i-1}{m-1}(\rho_2 - \rho_1), \quad \vartheta_j = \frac{2\pi(j-1)}{m},$$

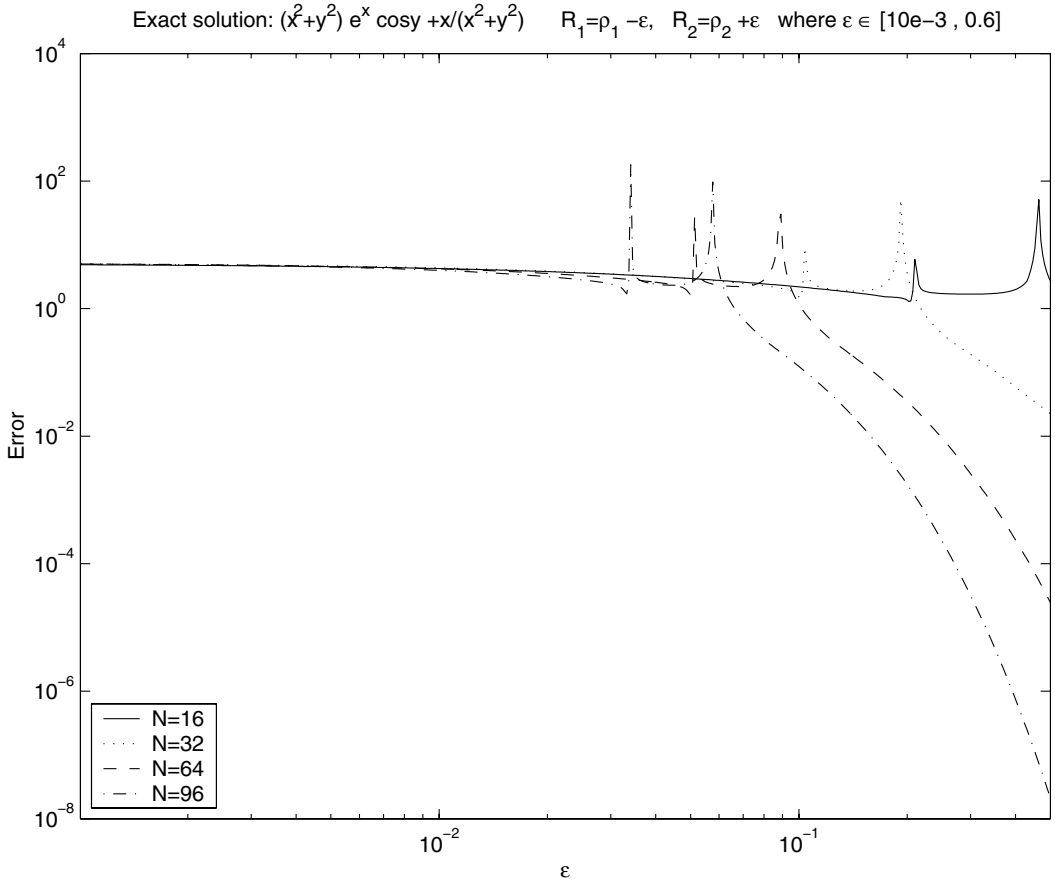

Figure 7 : Log–plot of maximum relative error versus ε in Example 3 for different values of N.

where $i, j = 1, \ldots, m$. The parameter m was taken to be equal to 21.

In Figures 1–4, we varied the angular parameter α and examined how this affected the accuracy of the solution for various values of N for different $\varepsilon = \rho_1 - R_1 = R_2 - \rho_2$. The numerical results indicate that for small ε, the accuracy of the solution is dependent on the angular parameter α. As ε grows this dependence disappears. Further, for a certain range of values of ε, the approximate solution is most accurate for $\alpha \approx \frac{1}{4}$. This phenomenon was also observed in Smyrlis and Karageorghis (2001, 2003, 2004b) and is valid for all the examples considered in this paper. (See Figures 1–4). We also varied the radii R_1 and R_2 which define the circles of the pseudo–boundary for $\alpha = 0$ and examined how this affected the accuracy of the solution for various values of N. In this case, we observed that as ε increases, the accuracy of the method improves. See Figures 5–8.

It has been observed that in certain cases two peaks appear for each value of N (see Figures 6–7). Numerical experimentation revealed that these are due to the fact that some of the 4×4 matrices defined in (3.3) are singular. The theoretical investigation of this singularity is beyond the scope of this paper but it should be noted that the full investigation of similar phenomena, for harmonic problems in a disk, can be found in Smyrlis and Karageorghis (2004b). The reason for which peaks do not appear in Figures 5 and 8, is that the examples in question have zero average on both boundaries. Therefore, the contributions of the eigenvectors corresponding to the vanishing eigenvalues of the global matrix are, in these examples, zero vectors.

Similar results were observed for $\alpha \neq 0$.

Finally, we varied the radius R_2 of the external circle of the pseudo–boundary keeping R_1 fixed and equal to $1/2$. We examined how this affected the accuracy of the approximation of the solution for various values of N. The results of Figures 9–12 indicate that as R_2 increases

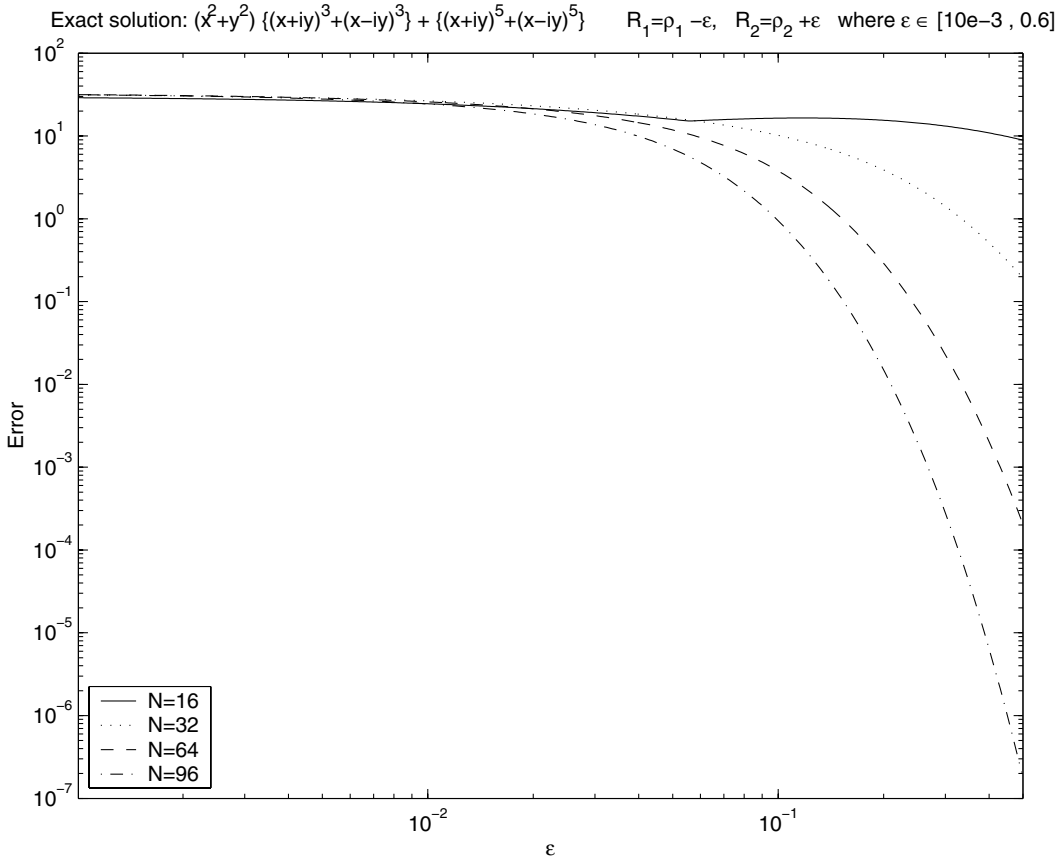

Figure 8 : Log–plot of maximum relative error versus ε in Example 4 for different values of N.

the accuracy improves. However, for larger values of ε the accuracy deteriorates. This phenomenon is due to ill-conditioning and has been repeatedly reported in the literature; see Kitagawa (1988, 1991); Ramachandran (2002); Smyrlis and Karageorghis (2001, 2003, 2004b). In particular, as the radius R_2 of the external circle of the pseudo–boundary increases, the values of the eigenvalues of the submatrices A_{mn}, $m,n = 1,\ldots,4$, range from $O(1)$ to $O\big((\frac{\rho_2}{R_2})^{N/2}\big)$. (See Smyrlis and Karageorghis (2004b).) Such small values cannot be captured numerically and this leads to ill–conditioning of the submatrices and hence of the global matrix in the linear system (2.13). The consequences of this ill–conditioning can be observed from Figures 9–12, where the error increases for large values of R and in some cases it is even impossible to solve the linear systems.

It should be noted that the way the closeness of the sources to the boundary affects the accuracy of the solution, depends on the number of boundary points. In Figures 5–12 one may observe that the accuracy of the method is poor for small values of $\varepsilon = R - \rho$, whereas it improves dramatically for $\varepsilon > 2\pi/N$. Similar phenomena were observed for the harmonic case in Tsangaris, Smyrlis, and Karageorghis (2004).

5 Conclusions

In this work, we develop an efficient algorithm for the solution of biharmonic problems in annular domains. This algorithm is based on a matrix decomposition formulation and exploits the circulant nature of the matrices involved by employing FFTs. The numerical results indicate that the accuracy of the solution is affected by the angle by which the singularities are rotated with respect to the boundary points and by the distance of the pseudo–boundary from the boundary of the annulus.

The ideas developed in this study could also be applied to different elliptic equations, such as the Helmholtz equation.

It should be noted that this approach has its limitations

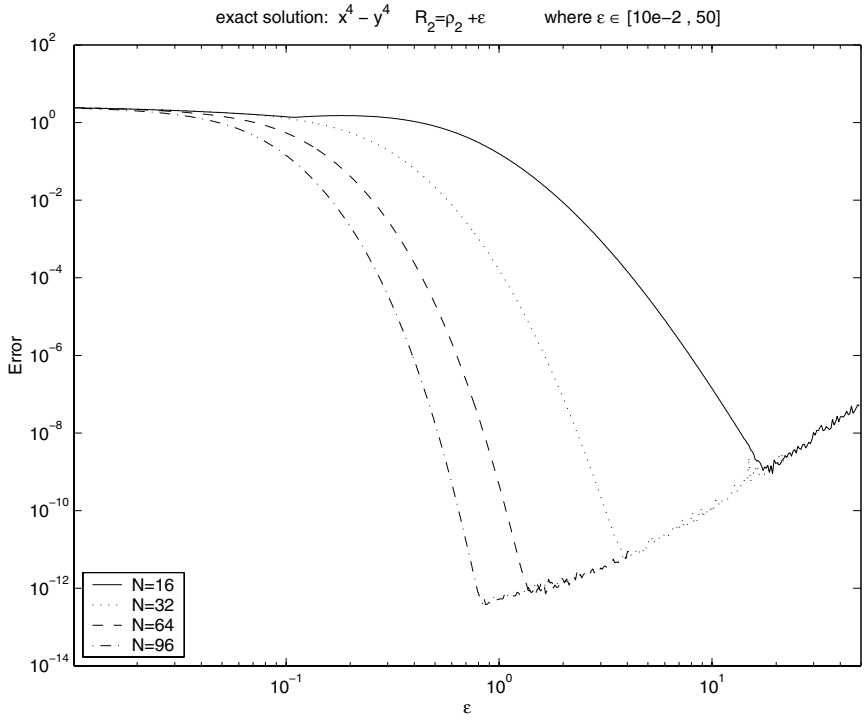

Figure 9 : Log–plot of maximum relative error versus ε in Example 1 for different values of N.

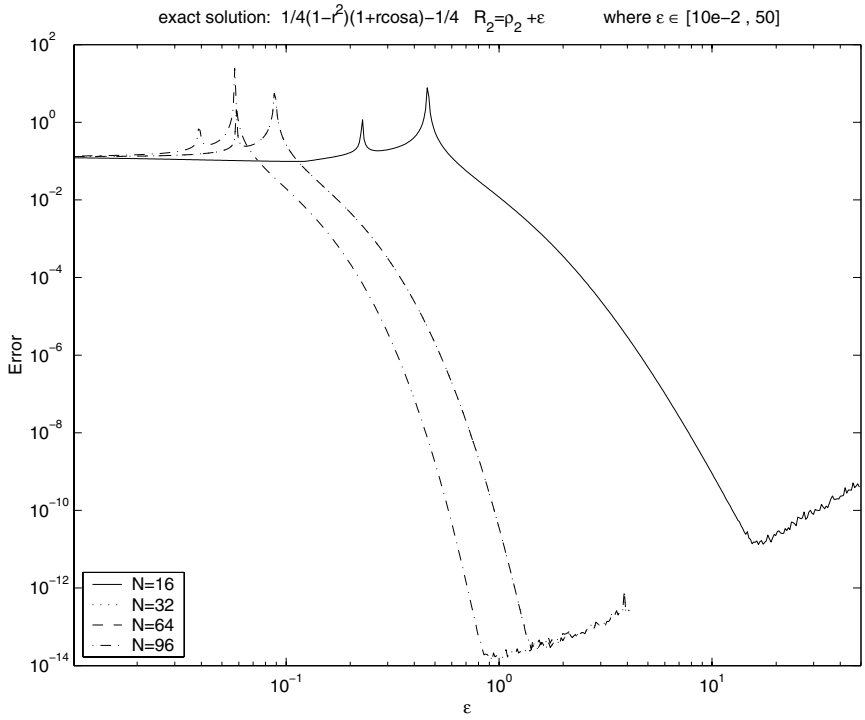

Figure 10 : Log–plot of maximum relative error versus ε in Example 2 for different values of N.

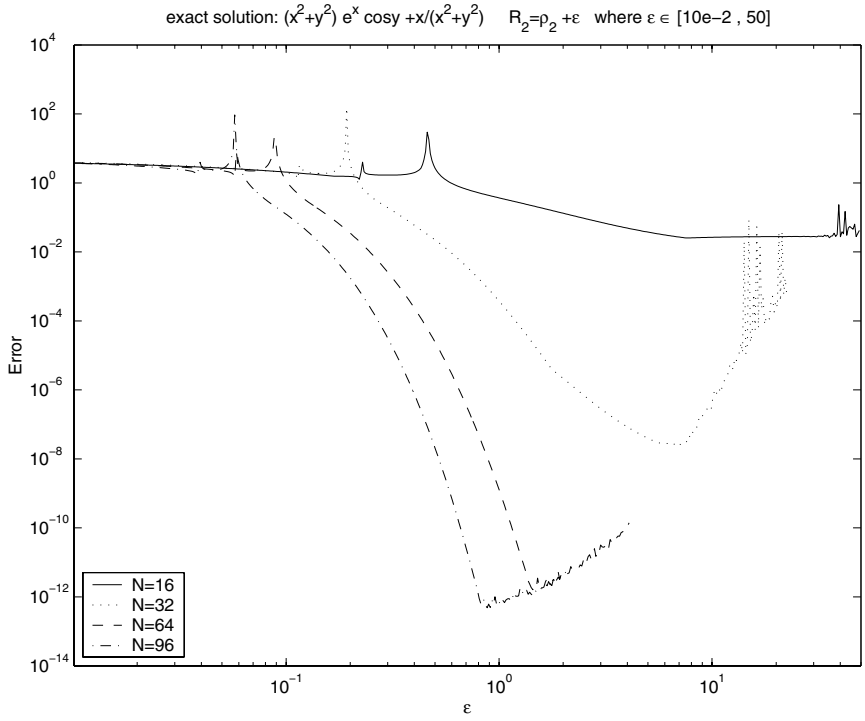

Figure 11 : Log–plot of maximum relative error versus ε in Example 3 for different values of N.

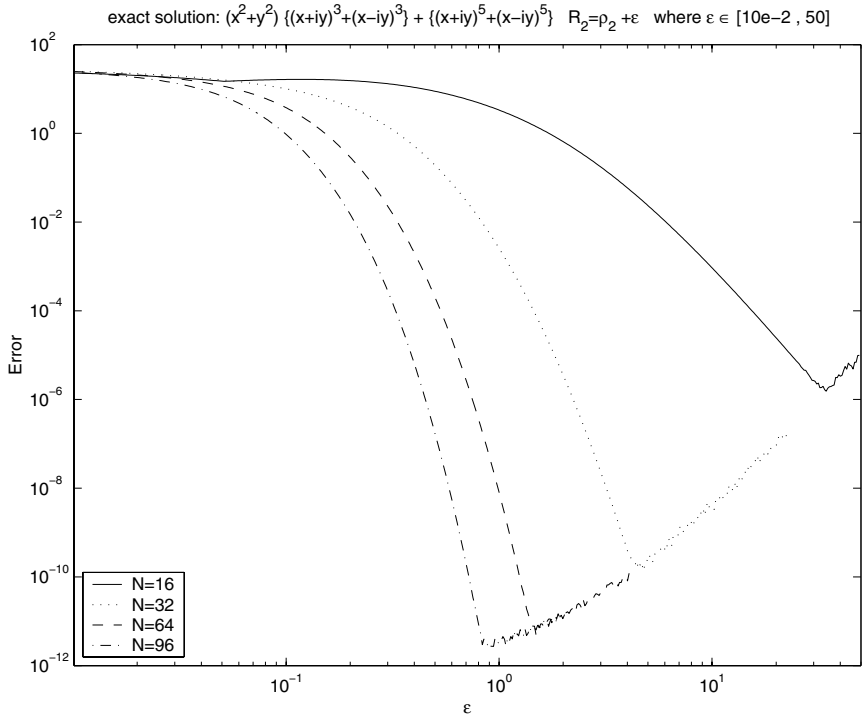

Figure 12 : Log–plot of maximum relative error versus ε in Example 4 for different values of N.

in the sense that it is only applicable to circular and annular domains. However, these ideas can be applied to certain three–dimensional problems. In particular, one could extend this algorithm to axisymmetric multiply connected shell–type biharmonic problems, in the spirit of the work of Fairweather, Karageorghis, and Smyrlis (2004); Smyrlis and Karageorghis (2004a), by exploiting the circular symmetries about the axis of rotation. In this case, if we suppose that we have an N^2-point discretization of the boundary of the axisymmetric solid, a matrix decomposition algorithm would lead to the solution of N independent $4N \times 4N$ systems, where the elements $\lambda_i^{k\ell}$ in the coefficient matrix of system (3.3), are now replaced by $N \times N$ matrices. Thus instead of solving a system of order N^2 which requires $O\left(N^6\right)$ operations, one would only need to solve N independent system of order $4N$ with cost $O\left(N^4\right)$.

Acknowledgements

The authors wish to thank the two anonymous referees for their constructive comments.

References

Almansi, E. (1897): Sull' integrazione dell' equazione differenziale $\Delta^{2n} = 0$. *Annali di Mathematica Pura et Applicata, Series III*, vol. 2, pp. 1–51.

Bogomolny, A. (1985): Fundamental solutions method for elliptic boundary value problems. *SIAM J. Numer. Anal.*, vol. 22, no. 4, pp. 644–669.

Chen, J. T.; Lin, J. H.; Kuo, S. R.; Chyuan, S. W. (2001): Boundary element analysis for the Helmholtz eigenvalue problems with a multiply connected domain. *R. Soc. Lond. Proc. Ser. A Math. Phys. Eng. Sci.*, vol. 457, no. 2014, pp. 2521–2546.

Cho, H. A.; Golberg, M. A.; Muleshkov, A. S.; Li, X. (2004): Trefftz methods for time dependent partial differential equations. *Comput. Mat. Cont.*, vol. 1, no. 1, pp. 1–37.

Davis, P. J. (1979): *Circulant matrices*. John Wiley & Sons, New York-Chichester-Brisbane. A Wiley-Interscience Publication, Pure and Applied Mathematics.

Fairweather, G.; Karageorghis, A. (1998): The method of fundamental solutions for elliptic boundary value problems. Numerical treatment of boundary integral equations. *Adv. Comput. Math.*, vol. 9, no. 1-2, pp. 69–95.

Fairweather, G.; Karageorghis, A.; Martin, P. A. (2003): The method of fundamental solutions for scattering and radiation problems. *Engng. Analysis with Boundary Elements*, vol. 27, pp. 759–769.

Fairweather, G.; Karageorghis, A.; Smyrlis, Y.-S. (2004): A matrix decomposition MFS algorithm for axisymmetric biharmonic problems. *Adv. Comput. Math.* To appear.

Fichera, G. (1961): Linear elliptic equations of higher order in two independent variables and singular integral equations, with applications to anistropic inhomogeneous elasticity. In Langer, R. E.(Ed): *Partial differential equations and continuum mechanics*, pp. 55–80. Univ. of Wisconsin Press, Madison, Wis.

Golberg, M. A.; Chen, C. S. (1997): *Discrete projection methods for integral equations*. Computational Mechanics Publications, Southampton.

Golberg, M. A.; Chen, C. S. (1999): The method of fundamental solutions for potential, Helmholtz and diffusion problems. In *Boundary integral methods: numerical and mathematical aspects*, volume 1 of *Comput. Eng.*, pp. 103–176. WIT Press/Comput. Mech. Publ., Boston, MA.

Golberg, M. A.; Chen, C. S. (2001): A mesh–free method for solving nonlinear reaction–diffusion equations. *CMES: Computer Modeling in Engineering & Sciences*, vol. 2, no. 1, pp. 87–92.

Karageorghis, A.; Fairweather, G. (1987): The method of fundamental solutions for the numerical solution of the biharmonic equation. *J. Comput. Phys.*, vol. 69, no. 2, pp. 434–459.

Karageorghis, A.; Fairweather, G. (1988): The Almansi of fundamental solutions for solving biharmonic problems. *Internat. J. Numer. Methods Engrg.*, vol. 26, pp. 1668–1682.

Karageorghis, A.; Fairweather, G. (1989): The simple layer potential method of fundamental solutions for certain biharmonic problems. *Internat. J. Numer. Methods Fluids*, vol. 9, no. 10, pp. 1221–1234.

Katsurada, M.; Okamoto, H. (1988): A mathematical study of the charge simulation method. I. *J. Fac. Sci. Univ. Tokyo Sect. IA Math.*, vol. 35, no. 3, pp. 507–518.

Kitagawa, T. (1988): On the numerical stability of the method of fundamental solution applied to the Dirichlet problem. *Japan J. Appl. Math.*, vol. 5, no. 1, pp. 123–133.

Katsurada, M. (1989): A mathematical study of the charge simulation method. II. *J. Fac. Sci. Univ. Tokyo Sect. IA Math.*, vol. 36, no. 1, pp. 135–162.

Kitagawa, T. (1991): Asymptotic stability of the fundamental solution method. *J. Comput. Appl. Math.*, vol. 38, no. 1-3, pp. 263–269. Proceedings of the International Symposium on Computational Mathematics (Matsuyama, 1990).

Kołodziej, J. A. (2001): *Applications of the Boundary Collocation Method in Applied Mechanics*. Wydawnictwo Politechniki Poznańskiej, Poznań. In Polish.

Kuo, S. R.; Chen, J. T.; Huang, C. X. (2000): Analytical study and numerical experiments for true and spurious eigensolutions of a circular cavity using the real–part dual BEM. *Int. J. Numer. Meth. Engng.*, vol. 48, pp. 1401–1422.

Kupradze, V. D.; Aleksidze, M. A. (1963): An approximate method of solving certain boundary-value problems. *Soobšč. Akad. Nauk Gruzin. SSR*, vol. 30, pp. 529–536.

Kupradze, V. D.; Aleksidze, M. A. (1964): The method of functional equations for the approximate solution of certain boundary-value problems. *Ž. Vyčisl. Mat. i Mat. Fiz.*, vol. 4, pp. 683–715.

Kuwahara, K.; Imai, I. (1969): Steady, viscous flow with circular boundary. *Phys. Fluids Supple.*, vol. 12, no. II-94–II-101.

Maiti, M.; Chakrabarty, S. K. (1974): Integral equation solutions for simply supported polygonal plates. *Int. J. Engng. Sci.*, vol. 12, no. 10, pp. 793–806.

Mathon, R.; Johnston, R. L. (1977): The approximate solution of elliptic boundary-value problems by fundamental solutions. *SIAM J. Numer. Anal.*, vol. 14, no. 4, pp. 638–650.

Murashima, S.; Nonaka, Y.; Nieda, H. (1983): The charge simulation method and its applications to the two–dimensional elasticity. In Brebbia, C. A.; Futagami, T.; Tanaka, M.(Eds): *Boundary elements. Proceedings of the fifth international conference on boundary element methods held in Hiroshima, November, 1983*, pp. 75–80. Springer-Verlag, Berlin.

Ramachandran, P. A. (2002): Method of fundamental solutions: singular value decomposition analysis. *Commun. Numer. Meth. Engng.*, vol. 18, pp. 789–801.

Smyrlis, Y.-S.; Karageorghis, A. (2001): Some aspects of the method of fundamental solutions for certain harmonic problems. *J. Sci. Comput.*, vol. 16, no. 3, pp. 341–371.

Smyrlis, Y.-S.; Karageorghis, A. (2003): Some aspects of the method of fundamental solutions for certain biharmonic problems. *CMES: Computer Modeling in Engineering & Sciences*, vol. 4, no. 5, pp. 535–550.

Smyrlis, Y.-S.; Karageorghis, A. (2004): A matrix decomposition MFS algorithm for axisymmetric potential problems. *Engng. Analysis with Boundary Elements*, vol. 28, pp. 463–474.

Smyrlis, Y.-S.; Karageorghis, A. (2004): Numerical analysis of the MFS for certain harmonic problems. *M2AN Math. Model. Num. Anal.*, vol. 28, no. 3, pp. 495–517.

Tsangaris, T.; Smyrlis, Y.-S.; Karageorghis, A. (2004): Numerical analysis of the MFS for harmonic problems in annular domains. Technical Report TR–06–2004, Department of Mathematics and Statistics, University of Cyprus, 2004.